Computed tomographic (CT) reconstruction from limited projection angles

Kenneth M. Hanson
Hydrodynamics Group, Los Alamos National Laboratory
Mail Stop P912, Los Alamos, New Mexico 87545

Abstract

When the available CT projection data are incomplete, there exists a null space in the space of possible reconstructions about which the data provide no information. Deterministic CT reconstructions are impotent in regard to this null space. Furthermore, it is shown that consistency conditions based on projection moments do not provide the missing projections. When the projection data consist of a set of parallel projections that do not encompass a complete 180° rotation, the null space corresponds to a missing sector in the Fourier transform of the original 2-D function. The long-range streak artifacts created by the missing sector can be reduced by attenuating the Fourier transform of the reconstruction smoothly to zero at the sector boundary. It is shown that the Fourier transform of a reconstruction obtained under a maximum entropy constraint is nearly zero in the missing sector. Hence, maximum entropy does not overcome the basic lack of information. It is suggested that some portion of the null space might be filled in by use of *a priori* knowledge of the type of image expected.

Introduction

The problem of CT reconstruction from a limited number of projections that do not encompass a complete 180° rotation continues to be an important one. There are a number of applications in which only limited angular data are available. Examples in 2-D include gated heart studies[1] and suitcases travelling on conveyor belts.[2] In 3-D, limited data arise in seven pinhole camera[3] and rotating slant-hole collimator[4] studies in nuclear medicine. Practicality or expense is usually the principal reason for having a limited number of projections. Contrary to what several authors have stated, a reduced number of projections does not necessarily reduce patient dose since the detectability of lesions is related to the total number of detected quanta and hence the dose.[5]

In this paper we will first consider the limitations imposed upon deterministic reconstruction algorithms by an incomplete angular range of projection measurements. The nature of the types of artifacts produced by missing projections will be demonstrated and a method for reducing their influence presented. The usefulness of consistency conditions and other constraints in supplying missing projections will be discussed. A maximum entropy reconstruction will be shown to suffer from the expected limitations. The use of *a priori* knowledge about the type of reconstruction expected will be considered in closing.

Properties of deterministic solutions

We consider real, two-dimensional functions of limited spatial extent f(x,y). The i'th projection of this function is defined as

$$p_i = \int\int h_i(x,y) f(x,y) dxdy \qquad (1)$$

where h_i is a nonnegative response function that defines how much the value of f at each point contributes to the i'th projection. Typically h_i has large values in a narrow strip that crosses the support of f with small or zero values outside the strip. The index i ranges over all of the projection measurements available. Typically the measurements are assumed to be ordered so that if there are N measurements made for each view and M views, the first view corresponds to i = 1,2,...N, the second view to i = N+1,...,2N, etc. It is important to realize that out of the space of all acceptable functions f(x,y), the finite set of response functions h_i can only span a subspace called the measurement space *M*. There will in general be a sub-space orthogonal to *M* called the null space *N* such that if f^o belongs to *N*,

$$\int\int h_i(x,y) f^o(x,y) dxdy = 0 \qquad (2)$$

for all i. It is clear that if a solution $\hat{f}$ is found that satisfies the measurements, Eq. 1, any function f^o from the null space may be added to it and still satisfy the measurements. The measurements provide no information in regard to how to specify any of the functions belonging to *N*. In other words, the solution $\hat{f}$ is ambiguous with respect to the null space. Ghosts that can appear from the null space of a finite set of projection measurements have been studied by Louis.[6]

Because the h_i span the measurement space, it is always possible to represent a deterministic solution to Eq. 1 as

$$\hat{f}(x,y) = \sum_i a_i h_i(x,y) \tag{3}$$

This is the same form introduced by Buonocore, Brody and Macovski[7] for the purpose of facilitating faster reconstruction algorithms.[8] It is important to realize that solutions of the form of Eq. 3 do not admit any contribution from the null space. It is noted that Eq. 3 amounts to the backprojection process applied to a_i coefficients. Thus the filtered-backprojection[9] and ART[10] algorithms result in reconstruction of this form.

Substitution of Eq. 3 into Eq. 1 yields

$$p_i = \sum_j g_{ij} a_i \tag{4}$$

where

$$g_{ij} = \iint h_i(x,y) h_j(x,y)\,dxdy\ , \tag{5}$$

is called the gramian of the response functions. Equation 4 may be written in matrix notation as

$$P = GA \tag{6}$$

and the solution for the a_i's and hence $\hat{f}$ via Eq. 3 is

$$A = G^{-1}P \tag{7}$$

provided the gramian is nonsingular. This is the same as the fast minimum variance estimator presented by Buonocore et al.[8]

It is interesting to consider the eigenvectors of the gramian G. This leads to an expansion for $\hat{f}$ in terms of orthogonal functions that are linear combinations of the h_i.[11,12] Because G is positive-definite and symmetric, its eigenvalues are real and nonnegative. It is easily shown that in the presence of noisy measurements, the coefficients in the expansion become more difficult to determine as the corresponding eigenvalues decrease. The condition number of G, defined as the ratio of the maximum eigenvalue to the minimum eigenvalue, indicates the degree to which the solution is ill-conditioned. When the condition number becomes very large or infinite (G singular), solution may be had by adapting a constrained least-squares approach[11] or through the use of the pseudoinverse.[7] The eigenvalue map, where the gramian eigenvalues are ordered according to decreasing value, can provide an estimate of the number of independent degrees of freedom contained in the measurements (Eq. 1). In the case of a small number of widely-spaced projections, the number of degrees of freedom will not be much smaller than the number of measurements since the reconstruction is underdetermined.

Nature of artifacts in parallel projection geometry

A great simplification in the visualization of the CT problem occurs in the case of parallel projections, that is, when the response functions h_i associated with each view are parallel strips. This simplification arises because of the projection-slice theorem[13] which states that the 1-D Fourier transform of a parallel projection of f(x,y) is equal to the 2-D Fourier transform of f along a spoke through the zero-frequency origin oriented perpendicularly to the projection direction. We will ignore the slight deviations from this idealization that arise from the finite width and length of the h_i as well as from the discrete nature of the measurements. Then we may think of each projection as a measurement of the Fourier transform of f(x,y) along the corresponding spoke. The measurement space corresponds to the ensemble of spokes in the 2-D spatial frequency plane associated with the finite number of views. The null space corresponds to the remaining sectors. When the available measurements do not include a given range of angles, there will be a corresponding "missing sector" in Fourier space for which there is no information.

Because deterministic reconstruction algorithms use only the measurement space as a basis, e.g., Eq. 3, the resulting reconstructions essentially assume zero modulus for the Fourier transform of $\hat{f}$ in the missing sectors. In general, the original function will not have zero modulus there, so the reconstruction will possess artifacts because of the missing sector.

The type of artifacts to be expected may be demonstrated by way of a simple technique.[14] Figure 1 shows a phantom that was used by Inouye.[15] This image was filtered using a filter that is unity everywhere except in a 45° sector in which its value is zero, Fig. 2a. The result, Fig. 3a, shows the artifacts that would result from a deterministic reconstruction from a large number of parallel projections encompassing 135° rotation. Two effects are observed; a blurring in the direction perpendicular to the missing projection directions, and a fan-shaped streak artifact emanating from these blurred regions that covers the sector of missing projections. These artifacts have been observed many times before.[8,14,15,16] The annoying sharp-edged nature of the streaks may be eliminated by modifying the response of the filter so that it is smoothly tapered to zero at the missing sector boundary, Fig. 3b. This apodization also causes a slight increase in the blur already present in Fig. 3a. In Fig. 3c it is seen that the artifacts are greatly reduced if the proper low-frequency components are included in the missing sector.

Consistency and other constraints

We have seen that deterministic reconstructions from projection with limited angular coverage leads to objectionable artifacts because of the lack of contribution from the null space so as to reduce the artifacts in the reconstruction. We will consider a number of possible approaches.

One seemingly powerful approach to filling in missing views is the use of consistency required of the projections.[17] Consistency is normally based on the moments of the projections, the n'th moment of the j'th projected defined for parallel projections as

$$M_j^n = \sum_{i \varepsilon j} X_i^n P_i \tag{8}$$

where X_i is the distance of the center of h_i from the center of rotation and the sum is over only i's corresponding to the j'th projection. It is easy to show that

$$M_j^n \approx \int f(x,y) \left(x \cos\theta_j + y \sin\theta_j \right)^n dxdy \approx \sum_{m=0}^{n} b_{mn} \cos^{m-n}\theta_j \sin^n\theta_j \tag{9}$$

where θ_j is the angle of the j'th projection. This relation is an approximation only because of the finite width of the response functions h_i and the discrete nature of the projections. Given a set of M projections covering a certain limited range of angles, it is natural to consider obtaining the b_{mn} coefficients up to n = M-1. M-1 moments are determined for all angles and the projections at missing angles may be estimated. It has been shown by Peres[18] in an explicit example that this method does not recover structure that would only be seen by missing views. Reconstructions based on the same approach by Louis[19] also show the expected artifacts. The reason for these failures can be seen if the reconstruction estimate $\hat{f}$ (Eq. 3) is substituted into Eq. 9. The same angular dependence for M_j^n is obtained even though $\hat{f}$ does not contain any contribution from the null space. Thus, we see that if $\hat{f}$ satisfies the projection measurements, Eq. 1, the above procedure simply provides projections at other angles that are consistent with the measurement space solution. No new information concerning the null space is obtained.

Another approach to filling in the missing views is to exploit the analyticity of the Fourier transform of f, F(u,v). This analyticity assures us that we may express F(u,v) as an infinite power series in u and v. If this could be done in practice, it would be possible to determine F(u,v) throughout the u,v plane. Unfortunately, the series must be terminated since only a finite number of measurements are available. Furthermore, the measurements are always subject to noise, which experience has taught us is disastrous for any interpolation or extrapolation scheme. Nonetheless, Inouye has attempted to interpolate the Fourier transforms of the projections of Fig. 1 taken over a limited angular range to recover the missing views.[15] His results for noiseless projection data are not very encouraging. However, he showed that reasonably accurate estimates of the missing Fourier amplitudes could be obtained for low radial frequencies. Thus, it may be possible that if the contributions at frequencies well within the missing sector are attenuated, as with the filter in Fig. 2c, a reasonable result, similar to Fig. 3c, could be obtained.

Yet a third approach to obtaining a reasonable reconstruction in the face of missing views is to place a global constraint on f. For example, if C(f) is some function of f, we might require that f be chosen to minimize

$$\int C(f)\,dxdy \ . \tag{10}$$

To do this we look for the minimum of the Lagrangian

$$\int C\Big(f(x,y)\Big)\,dxdy - \sum_i \lambda_i \left[p_i - \int h_i\ (x,y) f(x,y)\,dxdy\right] \tag{11}$$

Setting the derivative of this with respect to λ_i to zero simply yields the measurement equations, Eq. 1. More to the point, differentiation with respect to f leads to

$$C'(f) = \sum_i \lambda_i h_i(x,y) \tag{12}$$

The importance of this is that it fixes the form of the reconstruction. The λ_i are to be determined so that the measurement equations are satisfied. One particular choice for C(f) is the norm of f, $|f|^2$. It is immediately seen that Eq. 12 then becomes the same as Eq. 3. The expansion of $\hat{f}$ in terms of the response functions is the minimum norm solution! No contribution from the null space is forthcoming.

Many other reasonable choices for C(f) are possible. For example, because one of the objectionable features of the artifacts in Fig. 3a are the streaks, it might be reasonable to choose C(f) in such a way as to maximize the smoothness of the reconstruction. Thus one might use the norm of the gradient of f,

$$\left(\frac{\partial f}{\partial x}\right)^2 + \left(\frac{\partial f}{\partial y}\right)^2 ,$$

or the Laplacian,

$$\frac{\partial^2 f}{\partial x^2} + \frac{\partial^2 f}{\partial y^2} .$$

Another choice that leads to global smoothness is the entropy, C(f) = f lnf. From Eq. 12, the maximum entropy solution has the form

$$\ln \hat{f} = \sum_i \lambda_i h_i - 1 \tag{13}$$

A maximum entropy reconstruction algorithm MENT based on this approach was derived by Minerbo[20] for the case where the h_i are nonoverlapping strips. Then the reconstruction takes the form of a product of factors, one factor for each projection measurement. This follows from Eq. 13.

The MENT algorithm was used to obtain a reconstruction of the phantom shown in Fig. 1. Twenty parallel projections of the phantom were taken with 9° spacing. Each projection consisted of 101 samples across the width of the phantom. The reconstruction, Fig. 4, is a reasonable approximation to the original image but with streak artifacts arising from the sharp edges because of the limited number of views. Figure 5a shows the MENT reconstruction when only the first 15 views are used. The exclusion of the 45° range of angles results in artifacts similar to those in Fig. 3a. The modulus of the Fourier transform of this image, Fig. 5b, shows that the MENT algorithm has little contribution in the missing sector despite the fact that MENT is a nonlinear algorithm. However, the failure of MENT to overcome the limitations of the measurement space is not surprising in light of Eq. 13, which says that the logarithm of the MENT reconstruction is confined to the measurement space.

Multiplicative ART (MART) is known to tend towards a maximum entropy solution.[21] It would presumably produce a reconstruction with deficiencies similar to those of MENT. MART also suffers from errors produced by the "unnatural" square pixel representation in the ray sum and multiplicative backprojection processes necessary for its implementation.[20]

A Priori Knowledge

Because the problem of reconstruction from a limited range of angles does not appear to be solvable in terms of deterministic methods together with auxiliary constraints, we are led to consider probabilistic methods. These are based on a priori knowledge of what are the most probable distributions for f(x,y). For example, an informed observer would probably judge Fig. 3a to be "wrong" on the basis of his past experience. Images just don't look like that. Nevertheless, Fig. 3a is a bonafide image taken from the space of all possible f(x,y). So rejection of this reconstruction might not be correct. We see that a priori knowledge can be misleading.

One type of a priori knowledge might be that the image is a collection of specific shapes. For example, we might know that the image is a superposition of circular discs, as Fig. 1. Then the reconstruction could be expanded in terms of those shapes and the variable shape parameters and amplitudes determined from the projection measurements. Figure 1 could obviously be exactly reconstructed from two noiseless projections (since all the circles are of different size). If the actual image does not conform to the assumed expansion, however, severe artifacts will be generated. These artifacts would be reduced if a correction based upon the residuals between the projections of the fitted distribution and the actual measurements were applied. This correction reconstruction would clearly only affect the measurement space contribution to the fitted distribution.

Another type of a priori knowledge might be that the reconstruction is a sample from a well-defined ensemble of images. Reconstruction could then be based upon optimization of an ensemble statistic, for example, maximum a posteriori probability.[22] Alternatively, a finite Karhunen-Loeve expansion [23] could be performed as the first step of the procedure outlined in the preceding paragraph. These approaches might work well in situations where the images can be typified by a small number of parameters, e.g., seven pinhole images of the heart,[3] but would be difficult to apply to complex images, e.g., x-ray CT scans of the head.

A priori knowledge may exist about the permissible range of values for the function $f(x,y)$. The positivity constraint, $f(x,y) \geq 0$ is well known, but its usefulness in medical applications is doubtful. An interesting variation is when $f(x,y)$ is known to have a given region of support, i.e., $f(x,y) = 0$ outside of a given region. In such a case, it has been shown that a modified Gerchberg-Papoulis algorithm can significantly reduce the artifacts created by a limited range of viewing angles.[16,23-26] This technique definitely produces a contribution from the null space and hence is worth pursuing. It has yet to be shown how well the technique works in realistic situations where the measurements are subject to noise, and the region of support is large. Furthermore, the artifacts created by the assumption that $f(x,y)$ is zero where it may actually not be, need to be explored

Acknowledgments

The author acknowledges many fruitful discussions with George Wecksung, who has helped clarify many fuzzy ideas. Gerald Minerbo has also contributed a great deal of insight and supplied the MENT code as well. Credit is due to Robert Koeppe for the MENT computations. This work has been supported by the U. S. Department of Energy under Contract No. W-7405-ENG-36.

References

1. Nassi, M., et al., "A Method for Stop-Action Imaging of the Heart Using Gated Computed Tomography," IEEE Trans. Biomed Eng. BME-28, 116-122 (1981).
2. Rowan, W. H., et al., "Algorithms for Limited-Angle CT," presented at Int. Workshop on Phys. and Eng. in Medical Imaging, Asilomar, California, March 15-18, 1982.
3. Vogel, R. A. Kirch, D. L., LeFree, M. T., et al., "A New Method of Multiplanar Emission Tomography Using a Seven Pinhole Collimator and an Anger Camera," J. Nucl. Med. 19, 648-654 (1978).
4. Nalcioglu, O., Morton, M. E., and Milne, N., "Computerized Longitudinal Tomography With a Bilateral Collimator," IEEE Trans. Nucl. Sci. NS-27, 430-434 (1980).
5. Hanson, K. M., "Detectability in Computed Tomographic Images," Med. Phys. 6, 441-451 (1979).
6. Louis, A. K., "Ghosts in Tomography - The Null Space of the Radon Transform," Math. Meth. Appl. Sci. 3, 1-10 (1981).
7. Buonocore, H. B., Brody, W. R. and Macovski, A., "Natural Pixel Decomposition for Two-Dimensional Image Reconstruction," IEEE Trans. Biomed. Eng. BME-28, 69-78 (1981).
8. Buonocore, H. B., Brody, W. R., and Macovski, A., "Fast Minimum Variance Estimator for Limited Angle CT Image Reconstruction," Med. Phys. 8, 695-702 (1981).
9. Shepp, L. A., Logan, B. F., "The Fourier Reconstruction of a Head Section," IEEE Trans. Nucl. Sci. NS-21, 21-43 (1974).
10. Herman, G. T., Lent, A., "Iterative Reconstruction Algorithms," Comput. Biol. Med. 6, 273-294 (1976).
11. McCaughey, D. G., Andrews, H. C., "Degrees of Freedom for Projection Imaging," IEEE Trans. Acoust., Speech, Signal Processing ASSP-25, 63-73 (1977).
12. Llacer, J., "Theory of Imaging With a Very Limited Number of Projections," IEEE Trans. Nucl. Sci., NS-26, 598-602 (1979).
13. Bracewell, R. N., "Strip Integration in Radio Astronomy," Australian J. Phys. 9, 198-217 (1956).
14. Chiu, M. Y., et al., "Three-dimensional Radiographic Imaging With a Restricted View Angle," J. Opt. Soc. Am. 69, 1323-1333 (1979).
15. Inouye, T., "Image Reconstruction With Limited Angle Projection Data," IEEE Trans. Nucl. Sci. NS-26, 2666-2669 (1979).

16. Tam, K. C., Perez-Mendez, V., MacDonald, B., "Limited Angle 3-D Reconstruction from Continuous and Pinhole Projections," IEEE Trans. Nucl. Sci. NS-27, 445-458 (1980).
17. Ein-Gal, M., Rosenfeld, D., and Macovski, A., "The Consistency of the Shadow: An Approach to Preprocessing in Computerized Tomography," Proc. Stanford Conference on Computerized Tomography, Stanford, California (1974).
18. Peres, A., "Tomographic Reconstruction from Limited Angular Data," J. Comp. Assist. Tomo. 3, 800-803 (1979).
19. Louis, A. K., "Picture Reconstruction from Projections in Restricted Range," Math. Meth. in the Appl. Sci. 2, 209-220 (1980).
20. Minerbo, G., "MENT: A Maximum Entropy Algorithm for Reconstructing a Source from Projection Data," Comput. Graph. Imag. Process. 10, 48-68 (1979).
21. Lent, A., "A Convergent Algorithm for Maximum Entropy Image Restoration, With a Medical X-ray Application," Proc. SPSE Int. Conf. on Image Analysis and Evaluation, (R. Shaw, Ed.), pp. 249-257, Toronto, Canada, July 19-23, 1976.
22. Andrews, H. C., Hunt, B. R., Digital Image Restoration (Prentice-Hall, Englewood Cliffs, New York, 1977).
23. Rosenfeld, A., Kak, A. C., Digital Picture Processing (Academic Press, New York, 1976).
24. Tam, K. C., Perez-Mendez, V., "Limited-Angle 3-D Reconstructions Using Fourier Transform Iterations and Radon Transform Iterations," Opt. Eng. 20, 586-589 (1981).
25. Tam, K. C., Perez-Mendez, V., "Tomographical Imaging With Limited-Angle Input," J. Opt. Soc. Am. 71, 582-592 (1981).
26. Tam, K. C., Perez-Mendez, V., "Limits to Image Reconstruction From Restricted Angular Input," IEEE Trans. Nucl. Sci. NS-28, 179-183 (1981).
27. Sato, T., et al., "Tomographic Image Reconstruction from Limited Projections Using Iterative Revisions in Image and Transform Spaces," Appl. Opt. 20, 395-399 (1981).

Figures

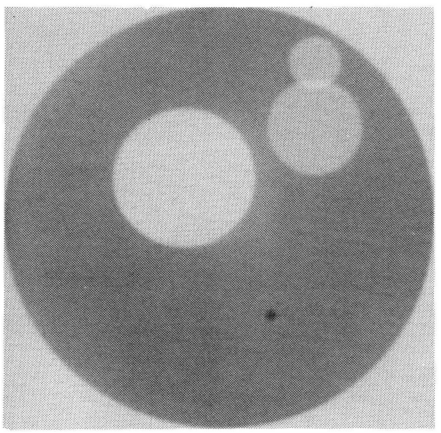

Figure 1. The phantom used in these studies. Taken from Inouye, this phantom has been smoothed slightly to avoid aliasing problems.

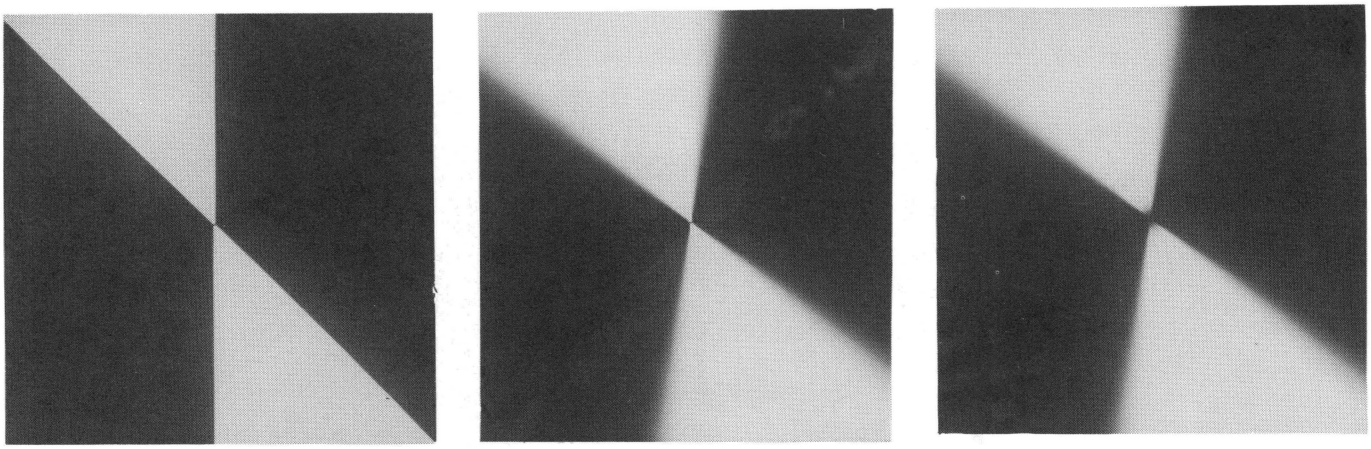

(a) (b) (c)

Figure 2. Display of the 2-D filters used to show the effect of CT reconstruction from parallel projections over a 135° angular range. Black corresponds to a filter value of unity; white to zero. In (a) the filter drops abruptly to zero at the missing sector boundary, whereas in (b) it is tapered to zero over a 15° wide sector. A small contribution in the missing sector at low frequencies is included in (c).

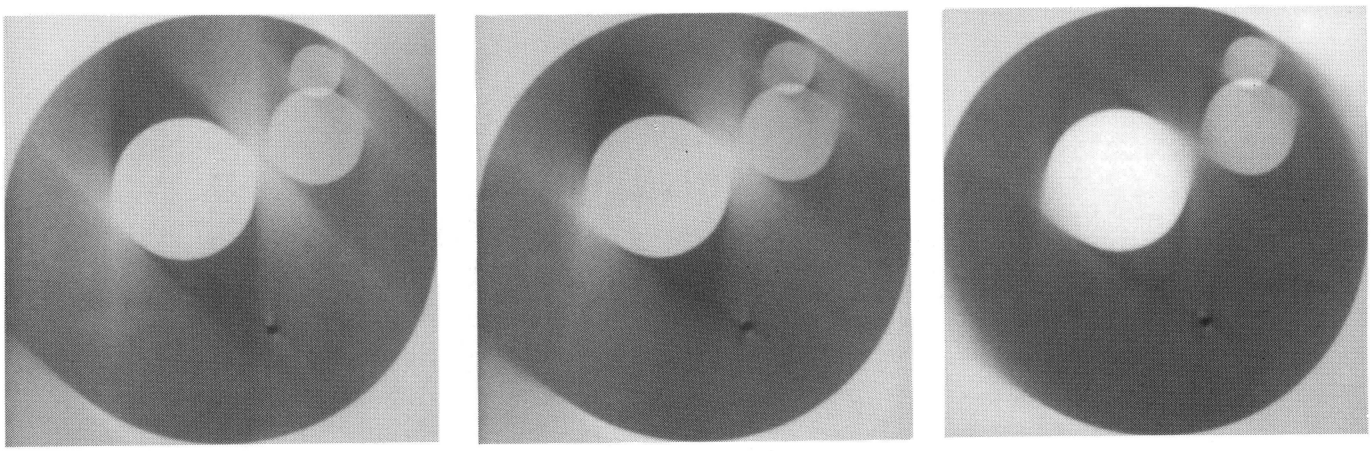

(a) (b) (c)

Figure 3. The results of applying the filters in Fig. 2 to the phantom of Fig. 1. Tapering the response at the sector boundary, (b), is seen to dramatically reduce the long-range streak artifacts at the expense of a slight increase in the blur in the direction perpendicular to the missing projections. The inclusion of low frequencies in the missing Fourier sector, (c), greatly improves the result.

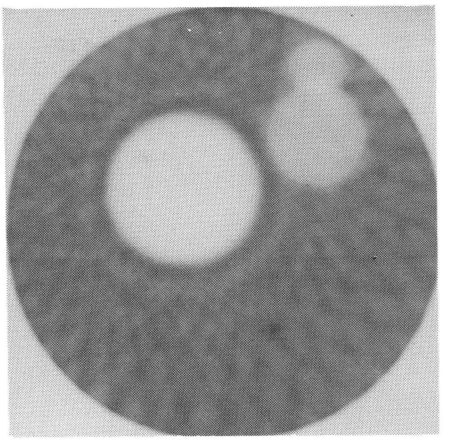

Figure 4. Reconstruction of the phantom from 20 equally spaced parallel projections covering 180° using a maximum entropy algorithm MENT.

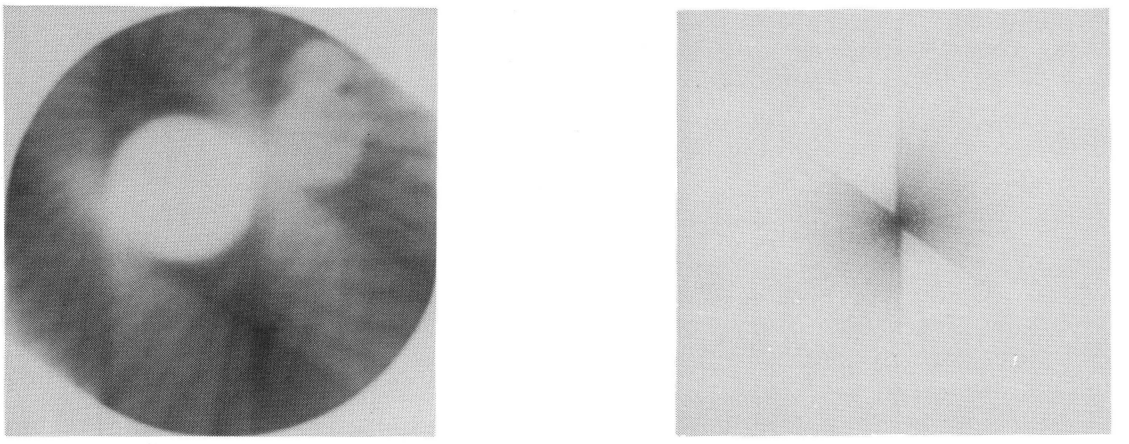

(a) (b)

Figure 5. (a) Reconstruction of the phantom from 15 views covering 135° using MENT. (b) The logarithm of the modulus of the 2-D Fourier transform (4 decades) of (a) shows nearly zero response in the missing sector.